Myeloid cell-specific deletion of inducible nitric oxide synthase protects against smoke-induced pulmonary hypertension in mice

Marija Gredic, Cheng-Yu Wu, Stefan Hadzic, Oleg Pak, Rajkumar Savai, Baktybek Kojonazarov, Siddartha Doswada, Astrid Weiss, Andreas Weigert, Andreas Guenther, Ralf P. Brandes, Ralph T. Schermuly, Friedrich Grimminger, Werner Seeger, Natascha Sommer, Simone Kraut and Norbert Weissmann

ONLINE SUPPLEMENT

MATERIALS AND METHODS

Experimental design and cigarette smoke exposure

Adult male and female iNos LysM-Cre mice (Nos2$^{tm2904.1Arte}$Tg(CAG-flpe)2ArteLyz2$^{tm1(cre)Ifo}$/), 3-4 months old, and age and gender-matched wildtype (WT) controls (C57BL/6N, obtained from Charles River Laboratories, Sulzfeld, Germany) were randomly allocated to tobacco-smoke-exposed or unexposed group (room air). Thirteen animals per group were subjected to hemodynamic and lung function measurements, echocardiography, fluorescent molecular tomography combined with micro-computed tomography (FMT-µCT) and right heart morphometry. Lungs of animals from each experimental group were randomly allocated to be 1) either paraffin-embedded or cryopreserved or 2) used for either flow cytometry or RNA and protein isolation. N numbers for final analysis vary owing to technical reasons, such as incorrect placement of the catheter or the echocardiographic probe, or to the premature death of some animals. All animal experiments were approved by the regional board for animal welfare (Regierungspräsidium Giessen, Germany).

Mice were exposed to cigarette smoke as described previously [1] and sacrificed after 3 or 8 months.

Chronic hypoxia exposure

Adult male and female Nos2 LysM-Cre mice (Nos2$^{tm2904.1ArteTg}$(CAG-flpe)2ArteLyz2$^{tm1(cre)Ifo}$/), 3-4 months old, and age and gender-matched WT controls (C57BL/6N, obtained from Charles River Laboratories, Sulzfeld, Germany) were exposed to normobaric hypoxia (10% O2) or normobaric normoxia (21% O_2) in a ventilated chamber for 28 days. Experiments were approved by the regional board for animal welfare (Regierungspräsidium Giessen, Germany).

Echocardiography and FMT-µCT

FMT-µCT (FMT; VisEn Medical, Bedford, MA, USA) was performed with Annexin Vivo 750 (Cat# NEV11053; Perkin Elmer, Waltham, USA). Echocardiographic assessment of the right heart structure and function was done one day prior to sacrifice under isoflurane anaesthesia as described previously [2].

Lung function and hemodynamic measurements

For the assessment of lung function, mice were tracheotomized, connected to the FlexiVent mechanical ventilator and data-acquisition system (SCIREQ, Montreal, Canada) and ventilated with a tidal volume of 10ml/kg at a frequency of 150 breaths/min. Snapshot and QuickPrime perturbation were imposed, and pressure-volume loops were generated for assessment of mechanical properties of the respiratory system. Deep inflation was used as a recruitment manoeuvre. Hemodynamic measurements were performed after two to three times repeated lung function measurements, as previously reported [3].

Lung fixation,organ harvest and assessment of right ventricular hypertrophy

Prior to the lung fixation, bronchoalveolar lavage (BAL) was done by introducing and then collecting 700µl of phosphate buffered saline (PBS). This procedure was repeated three times. Then, lung fixation and organ harvesting were done as previously described [4]. After lung fixation, the heart was removed and the weight of the dissected RV and the left ventricle plus septum (LV+S) was deterimined. The Fulton index (RV weight/(LV+S)weight) was calculated as a measure of RV hypertrophy. No significant changes in (LV+S) weight occurred between groups.

Flow cytometry and cell sorting

Single-cell suspensions of cells found either in BAL fluid (BALF) or in the remaining homogenized mouse lung tissue were blocked with FcR blocking reagent (MiltenyiBiotec, Bergisch Gladbach, Germany) in 0.5% PBS-bovine serum albumin (BSA) for 20min, stained with fluorochrome-conjugated antibodies and analyzed on an LSR II/Fortessa flow cytometer or sorted using a FACS Aria III cell sorter (both from BD Biosciences, San Jose, CA, USA). Data were analyzed using FlowJoVx. All antibodies and secondary reagents were titrated to determine optimal concentrations. Comp-Beads (BD Biosciences, San Jose, CA, USA) were used for single-colour compensation to create multicolour compensation matrices. For gating, fluorescence minus one controls were used. The instrument calibration was controlled daily using Cytometer Setup and Tracking beads (BD Biosciences, San Jose, CA, USA). For characterization of lung alveolar and interstitial macrophages (presented in Figure 3) [5, 6], the following antibodies were used: anti-CD11b-BV605, anti-CD44-AlexaFluor700, anti-Ly6G-APC-Cy7 (BD Biosciences, San Jose, CA, USA), anti-CD45-Vio-Blu (MiltenyiBiotec, Bergisch Gladbach, Germany), anti-CD206 and anti-F4/80-PE-Cy7 (BioLegend, San Diego, CA, USA).

Alveolar and pulmonary vascular morphometry and design-based stereology

Alveolar and pulmonary vascular morphometry, as well as design-based stereology, were performed as previously reported [1] with slight modifications. For the stereological calculations, the volume of the left lung was determined using the buoyancy-based water displacement method [7].

Western Blot analysis

The sample preparation, SDS PAGE electrophoresis, transfer and incubation with primary and secondary antibody were performed as previously described [1], with subtle modifications. Primary antibodies were used as follows: phospho-ERK (p44/p42) (Cat#9101S, Cell Signaling Technology, Danvers, MA, USA) 1:1000; p44/p42 (Cat#9102S, Cell Signaling Technology, Danvers, MA, USA) 1:1000; iNOS (Cat#ab178945, Abcam, Cambridge, UK) 1:1000; β-actin (Cat# b8227, Abcam, Cambridge, UK), 1:20000.

Visualization was done using the Clarity ECL Western Blotting Substrate (Biorad, Hercules, CA, USA) and ChemiDoc Touch Imaging System (Biorad, Hercules, CA, USA).

Laser microdissection and automated Western Blot analysis

Laser microdissection was done as described previously with subtle modifications [8]. Briefly, cryopreserved, Tissue-tek (Sakura Finetek, Staufen, Germany) embedded lung tissue was cut into 12µm thick sections and mounted on membrane-coated glass slides. Sections were stained with haematoxylin (diluted 20:30 with distilled H_2O) for 1min, and dehydrated in the graded ethanol series. 100 vessels per sample were captured by laser microdissection (LMD6000, Leica Microsystems, Wetzlar, Germany) and collected in 30µl of 0.1X Sample buffer (ProteinSimple, San Jose, CA, USA) containing a cOmplete™ Mini EDTA-free Protease-Inhibitor-Cocktail (Roche, Basel, Switzerland). Samples were sonicated (3 times for 30 seconds) and further prepared and analysed using the chemiluminescent detection system of the Jess Simple Western™ platform (ProteinSimple, San Jose, CA, USA) according to the manufacturer´s instructions. Antibodies were used as follows: p-p44/p42 phospho-ERK (p44/p42) (Cat#9101S, Cell Signaling Technology, Danvers, MA, USA) 1:4 and p44/p42 (Cat#9102S, Cell Signaling Technology, Danvers, MA, USA), 1:40.

cDNA synthesis and quantitative PCR (qPCR) analysis

cDNA synthesis and qPCR analysis were done as previously reported [8]. Primer sequences are available upon request.

Isolation of murine pulmonary artery smooth muscle cells (PASMC)

PASMC were isolated from precapillary vessels of 12-16 week old C57BL/6NCrl mice modified from a previously reported protocol [9]. Primary cells were cultured for 5-7 days without passaging in PASMC growth medium (Smooth Muscle Cell Growth Medium 2 (PromoCell, Heidelberg, Germany) + 100µg/ml Normocin (InvivoGen, Vista Sorrento Pkwy San Diego, CA, USA) + 10% (v/v) fetal bovine serum (FBS, Sigma Aldrich, Munich, Germany)). Smooth muscle cells were identified by immunohistochemical staining with smooth muscle cell-specific α-actin and myosin antibodies and examining their morphology. The absence of endothelial cells was confirmed by staining with an antibody directed against von Willebrand factor.

Isolation and differentiation of murine bone marrow-derived macrophages (BMDM)

Tibiae and femora from 12-16 week old C57BL/6NCrl or Nos2$^{tm2904.1Arte}$Tg(CAG-flpe)2ArteLyz2$^{tm1(cre)Ifo}$/ mice were removed under sterile conditions. Isolation of the bone-marrow cells and their differentiation to macrophages was done according to the previously reported protocol [8]. Bone ends were cut off and the bone shafts were then flushed with a 24G needle on a 10ml syringe with PBS without Ca^{2+} and Mg^{2+} (PAN Biotech, Aidenbach, Germany). The harvested bone-marrow was collected in 50ml tubes and centrifuged for 5 min at 400×g at room temperature. Cells were resuspended in BMDM differentiation medium (DMEM/F12 with 10mM L-glutamine, 100IU/ml penicillin, and 100µg/ml streptomycin (all from Gibco, Thermo Fisher Scientific Inc. Waltham, MA, USA), 10% (v/v) FBS (Sigma Aldrich, Munich, Germany) and 35ng/ml recombinant mouse M-CSF (PeproTech, Hamburg, Germany)) and passed through 40µm cell strainer. Cells were counted using a Neubauer hemocytometer and the number was adjusted to $7.5x10^6$ cells/ml. 10ml of cell suspension was seeded per one 10cm non-tissue culture treated Petri dish and cultured in a humidified atmosphere of 5% CO_2 at 37 °C for 7 days, with the addition of 5ml of differentiation medium on day 3. After 7 days, cells were harvested using enzyme-free cell dissociation buffer, seeded at 10^6 cells/ml in the full BMDM culture medium (DMEM/F12 with 10mM L-glutamine, 100IU/ml penicillin, and 100µg/ml streptomycin (all from Gibco, Thermo Fisher Scientific Inc. Waltham, MA, USA) and 10% (v/v) FBS (Sigma Aldrich, Munich, Germany)), and stimulated overnight with 100U/mL IFN-γ (PeproTech, Hamburg, Germany) to prime them for the differentiation into M1 cells.

Next day, IFN-γ was removed and cells were treated with 10ng/ml LPS (Sigma-Aldrich, Munich, Germany) to obtain M1 macrophages, or with 100U/mL IL-4 (PeproTech, Hamburg, Germany) to elicit M2 cells, with or without 100μM L-NIL (Cayman Chemicals, Ann Arbor, MI, USA).

Cigarette smoke extract (CSE) preparation

100% CSE was prepared by vaporizing one 3R4F cigarette (Kentucky Tobacco Research & Development Center, Lexington, USA) within one minute in 10ml of DMEM/F12 (Gibco, Thermo Fisher Scientific Inc. Waltham, MA, USA) medium. Then, it was filtered through a 20μm filter, diluted with the culture medium to the final concentration applied in the experiment and used immediately (in the following 20 minutes) for the cell treatment.

Cell viability assay for CSE-treated macrophages

After 6h of CSE treatment, the new culture medium with 10% (v/v) alamarBlue Cell Viability Reagent (Thermo Fisher Scientific Inc. Waltham, MA, USA) was added. Cell viability was determined after 16h according to the manufacturer's instructions.

Co-cultures of macrophages and PASMC

For experiments with co-cultures of macrophages and PASMC (Figure 5a and 6c), BMDM were seeded at 10^6 cells/mL on Transwell Permeable supports (Corning, New York, NY, USA), differentiated into M1 or M2 cells as described or left in the naïve state. Then, appropriate experimental groups were treated with 1% CSE for 3h. In parallel, PASMC were seeded in 24-well plate dishes at 15.000 cells/well and starved for 24h in PASMC basal medium (PromoCell, Heidelberg, Germany) supplemented with 0.1% FBS. Immediately before co-culturing of these cells, the culture medium was changed for both cell types, and BrdU labelling solution (Roche, Basel, Switzerland) was added to the PASMC. After 6 or 24h, PASMC were fixed and proliferation assay was done according to the manufacturer's instructions. The absorbance of the samples was measured in a microplate reader at 370nm (reference wavelength: 492nm). O.D. value for each experimental sample was standardized to the baseline, i.e. the value measured in control PASMC (that were not co-cultured with macrophages). CSE-dependent proliferation was calculated by subtracting proliferation of CSE-untreated group from the proliferation in corresponding CSE-treated co-cultures.

The experiment focused on the role of IL-4 in the pro-proliferative signalling in co-cultures was done as described, except for 100U/ml of recombinant IL-4 (PeproTech, Hamburg, Germany)

added to the co-culture medium of appropriate experimental groups immediately before co-culturing.

Experiments with co-culture-conditioned medium (CM)

For experiments with co-culture CM (Figure 5c, and S5a, b), PASMC and BMDM were co-cultured as previously described. The co-culture CM was collected (after 6h for the experiment shown in Figure 5c, and 24h for the experiment shown in Figures S5b, c), centrifuged for 5 min at 14000×g and kept on -80°C until further use. CM from PASMC monoculture was collected to serve as the control. On the day of the experiment, co-culture CM was thawed and equilibrated to room temperature (RT), and then used as described in the following text for ERK inhibition experiment and for apoptosis and migration assay.

Experiments with Macrophage-CM

For experiments with macrophage conditioned medium (Figure S4b), BMDM were seeded at 10^6 cells/mL in 24-well plates and left overnight in a humidified atmosphere of 5% CO_2 at 37 °C. Macrophages were differentiated into M1 or M2 cells as described. After the treatment with 1% CSE for 3h, the medium was changed and macrophages were cultured for the additional 24h, after which period CM was collected.

PASMC were seeded in 24-well plate dishes at 15.000 cells/well and starved for 24h in PASMC basal medium (PromoCell, Heidelberg, Germany) supplemented with 0.1% FBS. Then, the medium was replaced by the fresh medium containing 1) BrdU labelling solution (Roche, Basel, Switzerland) and 2) 50% CM collected from macrophage monocultures as described. After 24h, proliferation was measured according to the manufacturer's instructions and the O.D. values were standardized to the appropriate baseline (PASMC treated with fresh BMDM medium instead of macrophage-CM).

ERK inhibition experiment

PASMC were seeded in 96-well plate dishes at 5000 cells/well and starved for 24h in PASMC basal medium (PromoCell, Heidelberg, Germany) supplemented with 0.1% FBS. Cells were pre-treated with DMSO or 100µM SCH772984 for 3h. Afterwards, the medium was replaced by a fresh medium containing 1) BrdU labelling solution (Roche, Basel, Switzerland), 2) either DMSO (solvent) or 100µM SCH772984 (Selleckchem, Houston, TX, USA) in DMSO, and 3) 50% of either co-culture CM (collected after 6h co-culturing) or control CM from PASMC

monocultures. After 24h, proliferation was measured according to the manufacturer's instructions. Values were standardized to the appropriate baseline (either DMSO+PASMC CM-treated cells or SCH772984 inhibitor+PASMC CM-treated cells). CSE-dependent proliferation was calculated by subtracting the proliferation in the group treated with CM from CSE-unexposed co-cultures from the proliferation in the corresponding group treated with CM from CSE-exposed co-cultures (e.g. M2 CSE CM-M2 CM; or M2 L-NIL CSE CM-M2 L-NIL CM).

Apoptosis assay

PASMC were seeded at a density of 5000 cells/well in 96 well plates. Apoptosis kinetic assay (Abcam, Cambridge, UK) was done according to the manufacturer's instruction and IncuCyte ZOOM (Essen BioScience, Ann Arbor, MI, USA) was used for visualization. CSE, previously reported to induce apoptosis of murine primary PASMC [8], was used as a pro-apoptotic signal.

Migration assay

PASMC were seeded in 24 well plates containing 2 Well Culture-Inserts (Ibidi, Fitchburg, WI, USA) at 18000 cells/well and left overnight (5% CO_2, 37°C). The next day, inserts were removed, cells were washed twice with PBS and treated with 50% of co-culture CM or control macrophage growth medium. Closure of the wound made by insert's removal was followed using IncuCyte ZOOM for 24h and results are given as the percentage of wound confluence.

Cytokine array and ELISA assays

CM from co-cultures was harvested after 24h, centrifuged and kept at -80°C. On the day of the experiment, 400µl of CM was thawed on ice and assayed using Proteome Profiler Mouse XL Cytokine Array (R&D Systems, Minneapolis, MN, USA) according to the manufacturer's instructions. ELISA assay for IL-4 (R&D Systems, Minneapolis, MN, USA), was done in duplicates and following manufacturer's instructions, with 50µl of CM (pre-thawed and equilibrated to the RT) per well.

Immunocytochemical staining of PASMC

Murine PASMC were seeded on collagen-coated glass coverslips and co-cultured with M2 macrophages as previously described. At the respective time-points, cells were pre-fixed with

2% paraformaldehyde (PFA) added in co-culturing medium for 5 minutes, and then fixed with 4% PFA for additional 15 minutes at RT. After washing with PBS, cells were permeabilized with ice-cold 100% methanol for 10 minutes at -20°C and rinsed with PBS. Blocking was done for 1h at RT using 5% BSA 0.3% TritonX in PBS, and slides were incubated overnight at 4°C with a phospho-p44/p42 antibody (Cat#4370, Cell Signaling Technology, Danvers, MA, USA, 1:200) diluted in 1% BSA 0.3% TritonX in PBS. Following day, slides were washed with PBS and incubated with a Cy3-labelled α-smooth muscle actin antibody (Cat#C6198, Sigma-Aldrich, Munich, Germany 1:400) and Alexa488-labelled goat anti-rabbit secondary antibody (Cat#A-11034, Thermo Fisher Scientific Inc. Waltham, MA, USA, 1:400) for 2h at RT. After washing in PBS, cells were counterstained with 2µg/ml Hoechst in PBS for 10 min. Slides were mounted using Fluoro Care Anti-Fade Mountant (Biocare Medical) and analysed by confocal microscopy. At least three images from randomly chosen fields were taken for analysis.

Immunofluorescent staining of murine lungs

For immunofluorescent staining of mouse lung sections for CD68 and iNOS, 3µm thick serial sections of paraffin-embedded lung tissue were deparaffinised, rehydrated and antigen retrieval was done using Rodent Decloaker (Biocare Medical, Pacheco, CA, USA). Non-specific antibody binding was avoided by incubation of sections in 10% BSA for 1 h and in Background Punisher (Biocare Medical, Pacheco, CA, USA) for 15 minutes at RT. Following overnight incubation with both primary antibodies for iNOS (Cat#3523, Abcam, Cambridge, UK, 1:50) and CD68 (Cat#NB100-683, Novus Biologicals, Littleton, CO, USA, 1:50) at 4°C, slides were washed 3 times with PBS pH 7.4 and incubated with fluorescently labelled secondary antibodies (Cat#A-11034 and A-21422, Thermo Fisher Scientific Inc. Waltham, MA, USA, 1:400) for 2h at RT. After washing in PBS, sections were counterstained with DAPI and mounted using Fluoro Care Anti-Fade Mountant (Biocare Medical, Pacheco, CA, USA).

SUPPLEMENTARY DISCUSSION

Distinctiveness of smoke-induced inflammatory milieu driving pulmonary vascular remodelling in COPD

Alveolar hypoxia resulting from the impairment of respiratory function has long since been considered the main cause of the pulmonary vascular remodelling seen in COPD patients.

Identification of M2 macrophages, which were previously implicated in the development of hypoxic PH [10-12] as a critical cell type driving smoke-induced pulmonary vascular remodelling may suggest that this pathological event is driven by similar, hypoxia-dependent mechanisms. However, myeloid cell type-specific iNOS knockout animals developed hypoxia-induced PH and RV hypertrophy similar to wild-type mice. Given the phenotypical plasticity of macrophages and the spectrum of activation states that these cells are able to acquire, it is not surprising that specific pathways can be activated and are preferentially involved in (pathological) signalling events underlying vascular remodelling, depending on external stimuli and the microenvironmental milieu such as the one present in cigarette-smoke exposed lungs. Additionally, our result is in line with the recent hypothesis that pulmonary vascular remodelling is an early pathological event in COPD that occurs prior to the alveolar destruction and resulting hypoxemia. In this regard, we previously showed that 8 months of tobacco-smoke exposure in mice did not lead to hypoxemia [1]. The proposed sequence of vascular remodelling and alveolar destruction is substantiated by evidence from animal models [1, 8, 13-15] and human tissues [16, 17]. Going deeper into the matter our study provides further substantial evidence for the existence of smoke-specific signalling events underlying the remodelling of the pulmonary vasculature, independent from alveolar destruction. Our findings, if transferable to the human situation, can have an impact on the development of new treatment strategies for COPD-PH.

iNOS as a modulator of inflammatory cell phenotype and composition in smoke-induced PH

The second important consequence of myeloid cell-specific iNOS deletion on the composition of inflammatory cell infiltrates is the preserved proportion of T-cells in the population of lung immune cells, as opposed to the situation in smoke-exposed WT mice, where the portion of T-cells in lung inflammatory infiltrates is increased. Although assessment of absolute numbers is difficult due to smoke-induced dynamic changes of most cell populations in lungs, this finding suggests that lungs of smoke-exposed knockout mice have decreased T-cell numbers. This is of interest as an increased number of T-cells has been implicated in other forms of PH [18-20] and found in perivascular inflammatory infiltrates of COPD patients [16, 21]. Macrophage derived-iNOS could influence endothelial activation and T-cell diapedesis, as described for the T-cell extravasation into tumours [22]. Alternatively, changes in T-cell populations might be the consequence of the still largely undeciphered impact of

macrophage-derived iNOS on T-cell differentiation and activity. However, as Lysozyme M also labels a small portion of T- and B-cells, a more specific mouse line will be valuable for the further investigation of this phenomenon [23].

Factors influencing the assessment of cell proliferation in a co-culture setup

Analysing results from our numerous experiments done using the same co-culturing protocol, we observed differences in the response of PASMC to the same stimulus (in this case, co-culturing with CSE-exposed M2 macrophages) between experiments. These differences can be explained by the fact that assessment of proliferation was done using a BrdU assay, a technique semi-quantitative in nature. Moreover, in such setups, slight variations can occur due to 1) small differences during the above-described isolation of mouse primary PASMC and BMDM, or 2) variations introduced during seeding of the cells. 3) The need for the synchronized growth of two different primary cell types can further aggravate possible subtle discrepancies. 4) The respective experiments were done several years apart and 5) small batch-to-batch differences in products such as FBS, IL-4 or M-CSF could also account for the observed changes. A varying amplitude of changes in proliferation measured by BrdU in similar experimental conditions is, however, in accordance with the literature [24-28].

LITERATURE

1. Seimetz, M., N. Parajuli, A. Pichl, F. Veit, G. Kwapiszewska, F.C. Weisel, K. Milger, B. Egemnazarov, A. Turowska, B. Fuchs, S. Nikam, M. Roth, A. Sydykov, T. Medebach, W. Klepetko, P. Jaksch, R. Dumitrascu, H. Garn, R. Voswinckel, S. Kostin, W. Seeger, R.T. Schermuly, F. Grimminger, H.A. Ghofrani, and N. Weissmann, *Inducible NOS inhibition reverses tobacco-smoke-induced emphysema and pulmonary hypertension in mice.* Cell, 2011. **147**(2): p. 293-305.
2. Kojonazarov, B., S. Hadzic, H.A. Ghofrani, F. Grimminger, W. Seeger, N. Weissmann, and R.T. Schermuly, *Severe Emphysema in the SU5416/Hypoxia Rat Model of Pulmonary Hypertension.* Am J Respir Crit Care Med, 2019. **200**(4): p. 515-518.
3. Pradhan, K., A. Sydykov, X. Tian, A. Mamazhakypov, B. Neupane, H. Luitel, N. Weissmann, W. Seeger, F. Grimminger, A. Kretschmer, J.P. Stasch, H.A. Ghofrani, and R.T. Schermuly, *Soluble guanylate cyclase stimulator riociguat and phosphodiesterase 5 inhibitor sildenafil ameliorate pulmonary hypertension due to left heart disease in mice.* Int J Cardiol, 2016. **216**: p. 85-91.
4. Hadzic, S., C.Y. Wu, M. Gredic, B. Kojonazarov, O. Pak, S. Kraut, N. Sommer, D. Kosanovic, F. Grimminger, R.T. Schermuly, W. Seeger, S. Bellusci, and N. Weissmann, *The effect of long-term doxycycline treatment in a mouse model of cigarette smoke-induced emphysema and pulmonary hypertension.* Am J Physiol Lung Cell Mol Physiol, 2021.
5. Schyns, J., F. Bureau, and T. Marichal, *Lung Interstitial Macrophages: Past, Present, and Future.* J Immunol Res, 2018. **2018**: p. 5160794.
6. Misharin, A.V., L. Morales-Nebreda, G.M. Mutlu, G.R. Budinger, and H. Perlman, *Flow cytometric analysis of macrophages and dendritic cell subsets in the mouse lung.* Am J Respir Cell Mol Biol, 2013. **49**(4): p. 503-10.
7. Scherle, W., *A simple method for volumetry of organs in quantitative stereology.* Mikroskopie, 1970. **26**(1): p. 57-60.
8. Seimetz, M., N. Sommer, M. Bednorz, O. Pak, C. Veith, S. Hadzic, M. Gredic, N. Parajuli, B. Kojonazarov, S. Kraut, J. Wilhelm, F. Knoepp, I. Henneke, A. Pichl, Z.I. Kanbagli, S. Scheibe, A. Fysikopoulos, C.Y. Wu, W. Klepetko, P. Jaksch, C. Eichstaedt, E. Grunig, K. Hinderhofer, M. Geiszt, N. Muller, F. Rezende, G. Buchmann, I. Wittig, M. Hecker, A. Hecker, W. Padberg, P. Dorfmuller, S. Gattenlohner, C.F. Vogelmeier, A. Gunther, S. Karnati, E. Baumgart-Vogt, R.T. Schermuly, H.A. Ghofrani, W. Seeger, K. Schroder, F. Grimminger, R.P. Brandes, and N. Weissmann, *NADPH oxidase subunit NOXO1 is a target for emphysema treatment in COPD.* Nat Metab, 2020. **2**(6): p. 532-546.
9. Marshall, C., A.J. Mamary, A.J. Verhoeven, and B.E. Marshall, *Pulmonary artery NADPH-oxidase is activated in hypoxic pulmonary vasoconstriction.* Am J Respir Cell Mol Biol, 1996. **15**(5): p. 633-44.
10. Abid, S., E. Marcos, A. Parpaleix, V. Amsellem, M. Breau, A. Houssaini, N. Vienney, M. Lefevre, G. Derumeaux, S. Evans, C. Hubeau, M. Delcroix, R. Quarck, S. Adnot, and L. Lipskaia, *CCR2/CCR5-mediated macrophage-smooth muscle cell crosstalk in pulmonary hypertension.* Eur Respir J, 2019. **54**(4).
11. Vergadi, E., M.S. Chang, C. Lee, O.D. Liang, X. Liu, A. Fernandez-Gonzalez, S.A. Mitsialis, and S. Kourembanas, *Early macrophage recruitment and alternative activation are critical for the later development of hypoxia-induced pulmonary hypertension.* Circulation, 2011. **123**(18): p. 1986-95.

12. Amsellem, V., S. Abid, L. Poupel, A. Parpaleix, M. Rodero, G. Gary-Bobo, M. Latiri, J.L. Dubois-Rande, L. Lipskaia, C. Combadiere, and S. Adnot, *Roles for the CX3CL1/CX3CR1 and CCL2/CCR2 Chemokine Systems in Hypoxic Pulmonary Hypertension.* Am J Respir Cell Mol Biol, 2017. **56**(5): p. 597-608.
13. Wright, J.L. and A. Churg, *Effect of long-term cigarette smoke exposure on pulmonary vascular structure and function in the guinea pig.* Exp Lung Res, 1991. **17**(6): p. 997-1009.
14. Ferrer, E., V.I. Peinado, M. Diez, J.L. Carrasco, M.M. Musri, A. Martinez, R. Rodriguez-Roisin, and J.A. Barbera, *Effects of cigarette smoke on endothelial function of pulmonary arteries in the guinea pig.* Respir Res, 2009. **10**: p. 76.
15. Wright, J.L., T. Ngai, and A. Churg, *Effect of long-term exposure to cigarette smoke on the small airways of the guinea pig.* Exp Lung Res, 1992. **18**(1): p. 105-14.
16. Peinado, V.I., J.A. Barbera, P. Abate, J. Ramirez, J. Roca, S. Santos, and R. Rodriguez-Roisin, *Inflammatory reaction in pulmonary muscular arteries of patients with mild chronic obstructive pulmonary disease.* Am J Respir Crit Care Med, 1999. **159**(5 Pt 1): p. 1605-11.
17. Santos, S., V.I. Peinado, J. Ramirez, T. Melgosa, J. Roca, R. Rodriguez-Roisin, and J.A. Barbera, *Characterization of pulmonary vascular remodelling in smokers and patients with mild COPD.* Eur Respir J, 2002. **19**(4): p. 632-8.
18. Pullamsetti, S.S., R. Savai, W. Janssen, B.K. Dahal, W. Seeger, F. Grimminger, H.A. Ghofrani, N. Weissmann, and R.T. Schermuly, *Inflammation, immunological reaction and role of infection in pulmonary hypertension.* Clin Microbiol Infect, 2011. **17**(1): p. 7-14.
19. Bonnet, S., G. Rochefort, G. Sutendra, S.L. Archer, A. Haromy, L. Webster, K. Hashimoto, S.N. Bonnet, and E.D. Michelakis, *The nuclear factor of activated T cells in pulmonary arterial hypertension can be therapeutically targeted.* Proc Natl Acad Sci U S A, 2007. **104**(27): p. 11418-23.
20. Tuder, R.M., B. Groves, D.B. Badesch, and N.F. Voelkel, *Exuberant endothelial cell growth and elements of inflammation are present in plexiform lesions of pulmonary hypertension.* Am J Pathol, 1994. **144**(2): p. 275-85.
21. SAETTA, M., S. BARALDO, L. CORBINO, G. TURATO, F. BRACCIONI, F. REA, G. CAVALLESCO, G. TROPEANO, C.E. MAPP, P. MAESTRELLI, A. CIACCIA, and L.M. FABBRI, *CD8 + ve Cells in the Lungs of Smokers with Chronic Obstructive Pulmonary Disease.* 1999. **160**(2): p. 711-717.
22. Sektioglu, I.M., R. Carretero, N. Bender, C. Bogdan, N. Garbi, V. Umansky, L. Umansky, K. Urban, M. von Knebel-Doberitz, V. Somasundaram, D. Wink, P. Beckhove, and G.J. Hammerling, *Macrophage-derived nitric oxide initiates T-cell diapedesis and tumor rejection.* Oncoimmunology, 2016. **5**(10): p. e1204506.
23. Ye, M., H. Iwasaki, C.V. Laiosa, M. Stadtfeld, H. Xie, S. Heck, B. Clausen, K. Akashi, and T. Graf, *Hematopoietic stem cells expressing the myeloid lysozyme gene retain long-term, multilineage repopulation potential.* Immunity, 2003. **19**(5): p. 689-99.
24. Liu, G., P. Hao, J. Xu, L. Wang, Y. Wang, R. Han, M. Ying, S. Sui, J. Liu, and X. Li, *Upregulation of microRNA-17-5p contributes to hypoxia-induced proliferation in human pulmonary artery smooth muscle cells through modulation of p21 and PTEN.* Respir Res, 2018. **19**(1): p. 200.
25. Kim, F.Y., E.A. Barnes, L. Ying, C. Chen, L. Lee, C.M. Alvira, and D.N. Cornfield, *Pulmonary artery smooth muscle cell endothelin-1 expression modulates the*

pulmonary vascular response to chronic hypoxia. Am J Physiol Lung Cell Mol Physiol, 2015. **308**(4): p. L368-77.

26. Shan, R., L. Chen, X. Li, H. Wu, Q. Liang, and X. Tang, *Hypoxia promotes rabbit pulmonary artery smooth muscle cells proliferation through a 15-LOX-2 product 15(S)-hydroxyeicosatetraenoic acid.* Prostaglandins Leukot Essent Fatty Acids, 2012. **86**(1-2): p. 85-90.
27. Das, M., N. Burns, S.J. Wilson, W.M. Zawada, and K.R. Stenmark, *Hypoxia exposure induces the emergence of fibroblasts lacking replication repressor signals of PKCzeta in the pulmonary artery adventitia.* Cardiovasc Res, 2008. **78**(3): p. 440-8.
28. Ten Freyhaus, H., E.M. Berghausen, W. Janssen, M. Leuchs, M. Zierden, K. Murmann, A. Klinke, M. Vantler, E. Caglayan, T. Kramer, S. Baldus, R.T. Schermuly, M.D. Tallquist, and S. Rosenkranz, *Genetic Ablation of PDGF-Dependent Signaling Pathways Abolishes Vascular Remodeling and Experimental Pulmonary Hypertension.* Arterioscler Thromb Vasc Biol, 2015. **35**(5): p. 1236-45.

FIGURE LEGENDS

Figure S1: *iNos* gene deletion in myeloid cells using iNos LysM-Cre driver line.

Bone-marrow-derived macrophages were isolated from wildtype (WT) and iNos LysM-Cre mice and polarized *in vitro* using either interferon (IFN)-γ and lipopolysaccharide (LPS) to elicit M1 polarization, or interleukin (IL)-4 to achieve an M2 phenotype. a) Expression of *iNos* gene in naïve, M1 and M2 macrophages, quantified by real-time PCR. Graph shows mean ± SEM. *p < 0.05. Two-way ANOVA (with Sidak´s multiple comparison post-hoc test) was used. b) Western blot quantification of iNOS protein levels in naïve (upper), M1 (middle) and M2 (lower panel) macrophages. Graphs show mean ± SEM. *p < 0.05. Unpaired t-test was used for statistical analysis. c) Representative images of lung sections from WT and iNos LysM-Cre mice stained for CD68 (red) and iNOS (green) and counterstained with DAPI (blue). Scale bar = 10 µm.

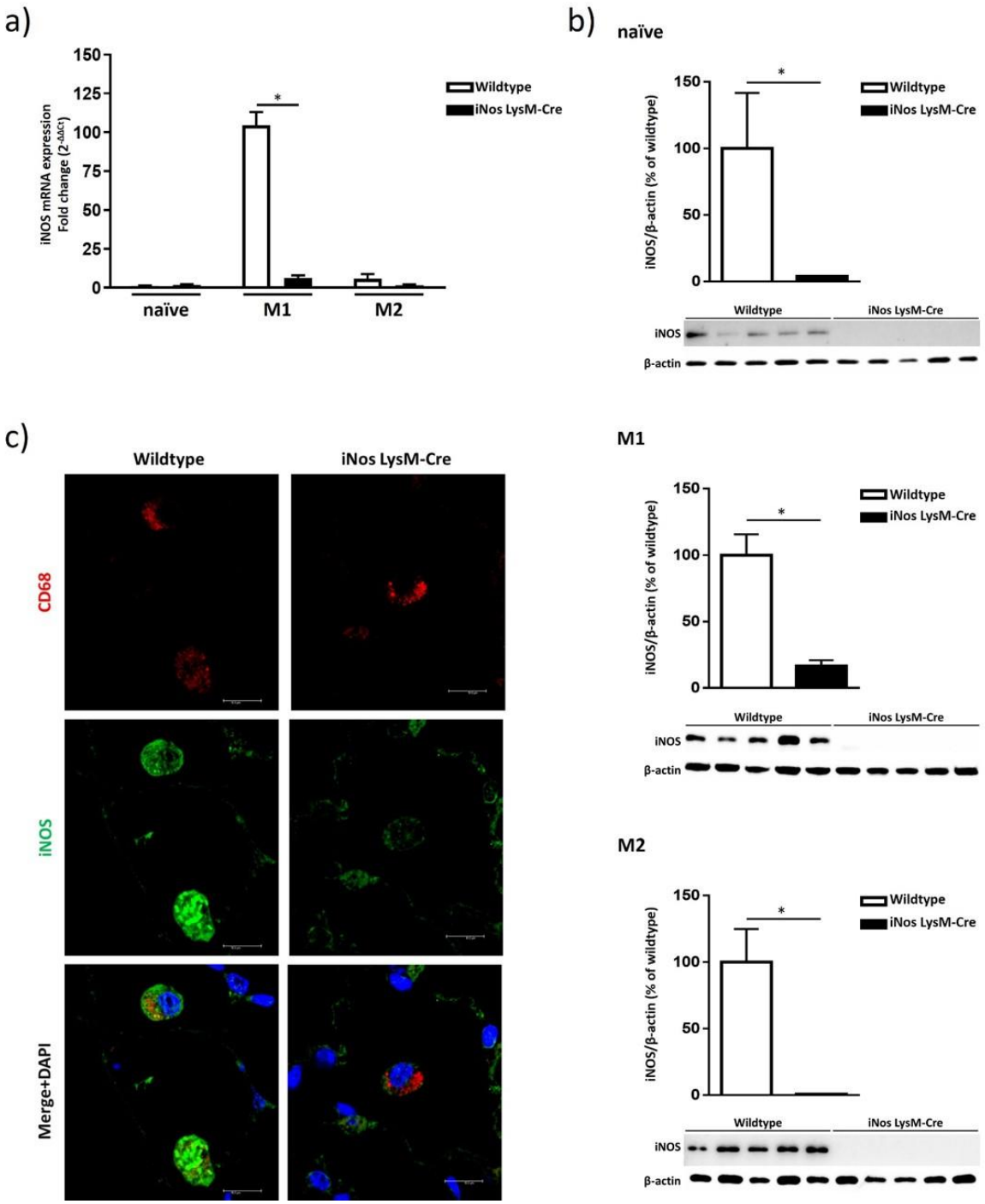
a)
iNOS mRNA expression
Fold change (2-ΔΔCt)
150
125
100
75
50
25
0
*
Wildtype
iNos LysM-Cre
naïve
M1
M2
b)
naïve
iNOS/β-actin (% of wildtype)
150
100
50
0
*
Wildtype
iNos LysM-Cre
Wildtype
iNos LysM-Cre
iNOS
β-actin
c)
Wildtype
iNos LysM-Cre
CD68
iNOS
Merge+DAPI
M1
iNOS/β-actin (% of wildtype)
150
100
50
0
*
Wildtype
iNos LysM-Cre
Wildtype
iNos LysM-Cre
iNOS
β-actin
M2
iNOS/β-actin (% of wildtype)
150
100
50
0
*
Wildtype
iNos LysM-Cre
Wildtype
iNos LysM-Cre
iNOS
β-actin

Figure S2: Analysis of lung structure after chronic smoke exposure

Wildtype and myeloid cell-specific iNOS knockout mice were exposed to smoke for 8 months. a) Tissue volume (left) and air/tissue ratio (right) in lungs of mice exposed to smoke for 8 months and respective unexposed (room air) controls (n=11-13), based on micro-computed tomography (µCT) imaging. b) Lung volume in mice after 8 months of smoke exposure, assessed by the water displacement method (n=7-9). c) Alveolar morphometry (n=6-7) showing the percentage of airspace (left), septal wall thickness (middle) and mean linear intercept (right) in mice after 8 months of smoke exposure. Graphs show mean ± SEM. *$p < 0.05$. Two-way ANOVA (with Tukey´s multiple comparison post-hoc test) was used. d) Representative images of lung sections from mice after 8 months of smoke exposure stained with haematoxylin-eosin (H&E). Scale bar = 100 µm.

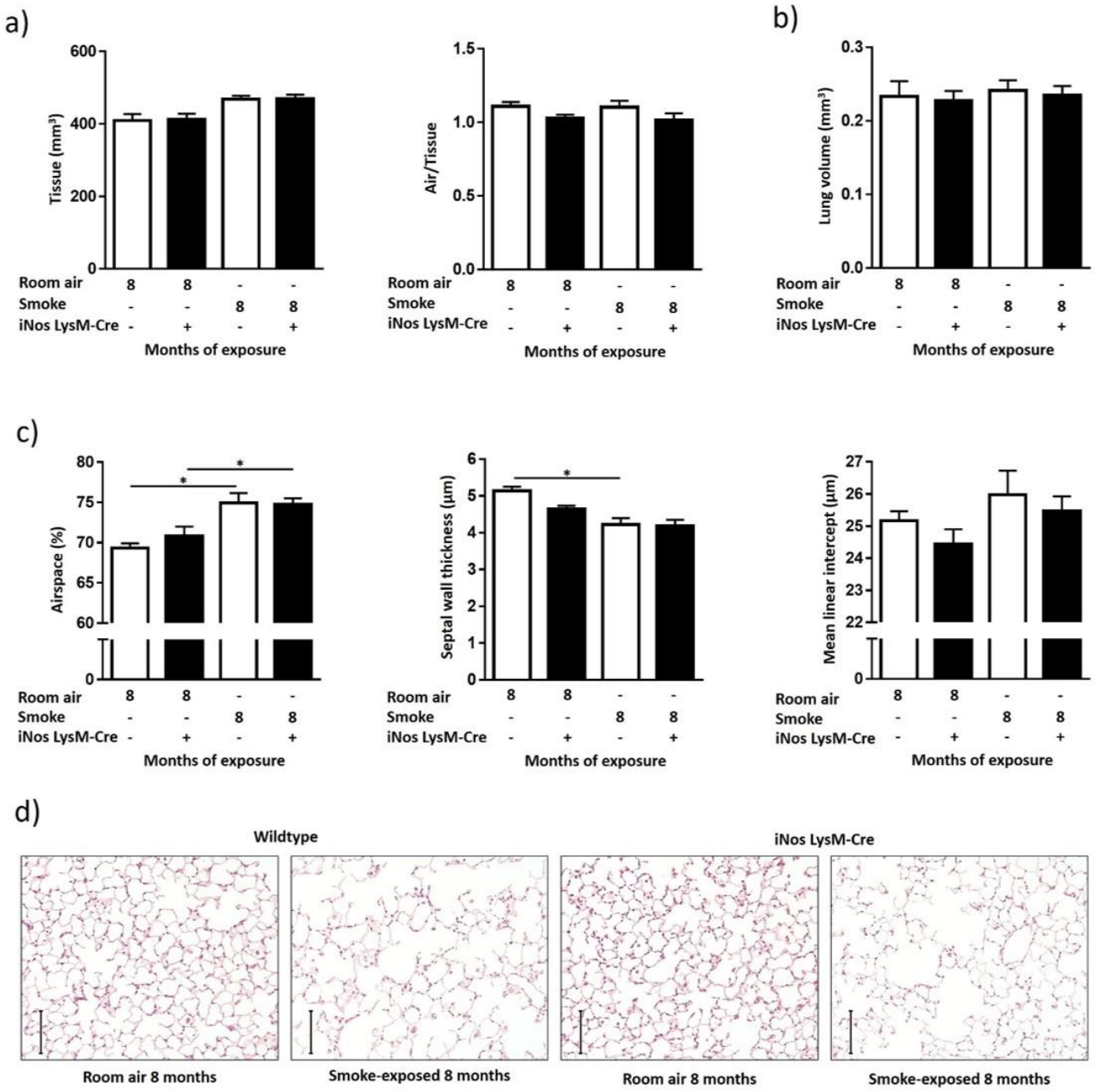
a)
Tissue (mm³)
600
400
200
0
Air/Tissue
1.5
1.0
0.5
0.0
b)
Lung volume (mm³)
0.3
0.2
0.1
0.0
Room air 8 8 - -
Smoke - - 8 8
iNos LysM-Cre - + - +
Months of exposure
c)
Airspace (%)
80
75
70
65
60
0
*
*
Septal wall thickness (µm)
6
5
4
3
2
1
0
*
Mean linear intercept (µm)
27
26
25
24
23
22
0
Room air 8 8 - -
Smoke - - 8 8
iNos LysM-Cre - + - +
Months of exposure
d)
Wildtype
iNos LysM-Cre
Room air 8 months
Smoke-exposed 8 months
Room air 8 months
Smoke-exposed 8 months

Figure S3: Flow cytometry analysis of T-cells in broncho-alveolar lavage fluid and lung homogenate of mice after 8 months of smoke exposure

a) $CD4^+$ T-lymphocytes and $CD8^+$ T-lymphocytes in lung homogenate. b) $CD4^+$ T-lymphocytes and $CD8^+$ T-lymphocytes found in the BALF (n=4-5). All values are given as the percentage of $CD45^+$ cells standardized to non-exposed control. Graphs show mean ± SEM. *$p < 0.05$. Statistical analysis was done by unpaired T-test.

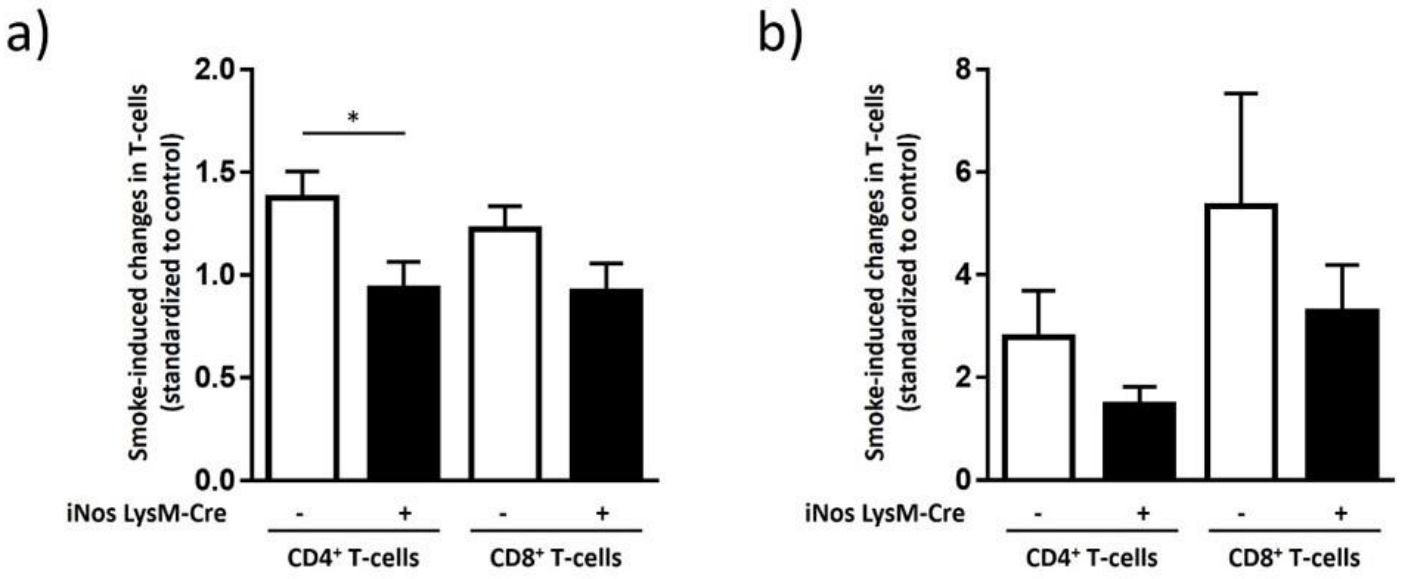

Figure S4: Analysis of smoke-induced changes in monocultures of bone marrow-derived macrophages

a) Metabolic activity of control, iNOS-deficient and L-NIL-treated M0, M1 and M2 macrophages after exposure to cigarette smoke extract (CSE), measured by alamarBlue assay and given as the percentage of control (n=6). b) Proliferation of mouse pulmonary artery smooth muscle cells (PASMC) during 24h of incubation with culture-conditioned medium from M1- (left) or M2- (right) polarized macrophages pre-treated with CSE, measured by BrdU incorporation assay and given as the percentage of control (n=4). Graphs show mean ± SEM. *$p < 0.05$. Two-way ANOVA (with Sidak´s multiple comparison post-hoc test) was used for statistical analysis.

a)

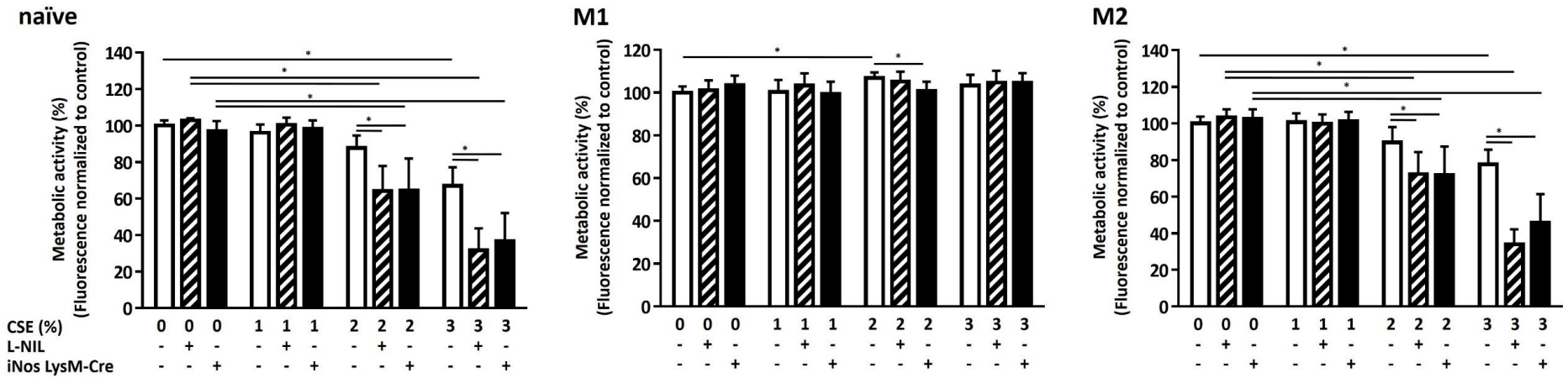
naïve
M1
M2
Metabolic activity (%)
(Fluorescence normalized to control)
CSE (%)
L-NIL
iNos LysM-Cre

b)


Proliferation (%)
(Absorbance normalized to control)
CSE (%)
L-NIL

Figure S5: Investigation of the effect of the crosstalk between macrophages and PASMC on migration and apoptosis of PASMC

a) Migration of PASMC treated with conditioned medium (CM) from co-cultures of PASMC and control or CSE and/or L-NIL-treated M2 macrophages (n=5). Data are given as the percentage of wound confluence. b) Apoptosis of PASMC treated with CM from co-cultures of PASMC and control or CSE and/or L-NIL-treated M2 macrophages (n=5), given as the confluence of cells labelled with annexin. Graphs show mean ± SEM. *p < 0.05. Two-way ANOVA (with Sidak´s multiple comparison post-hoc test) was used for statistical analysis.

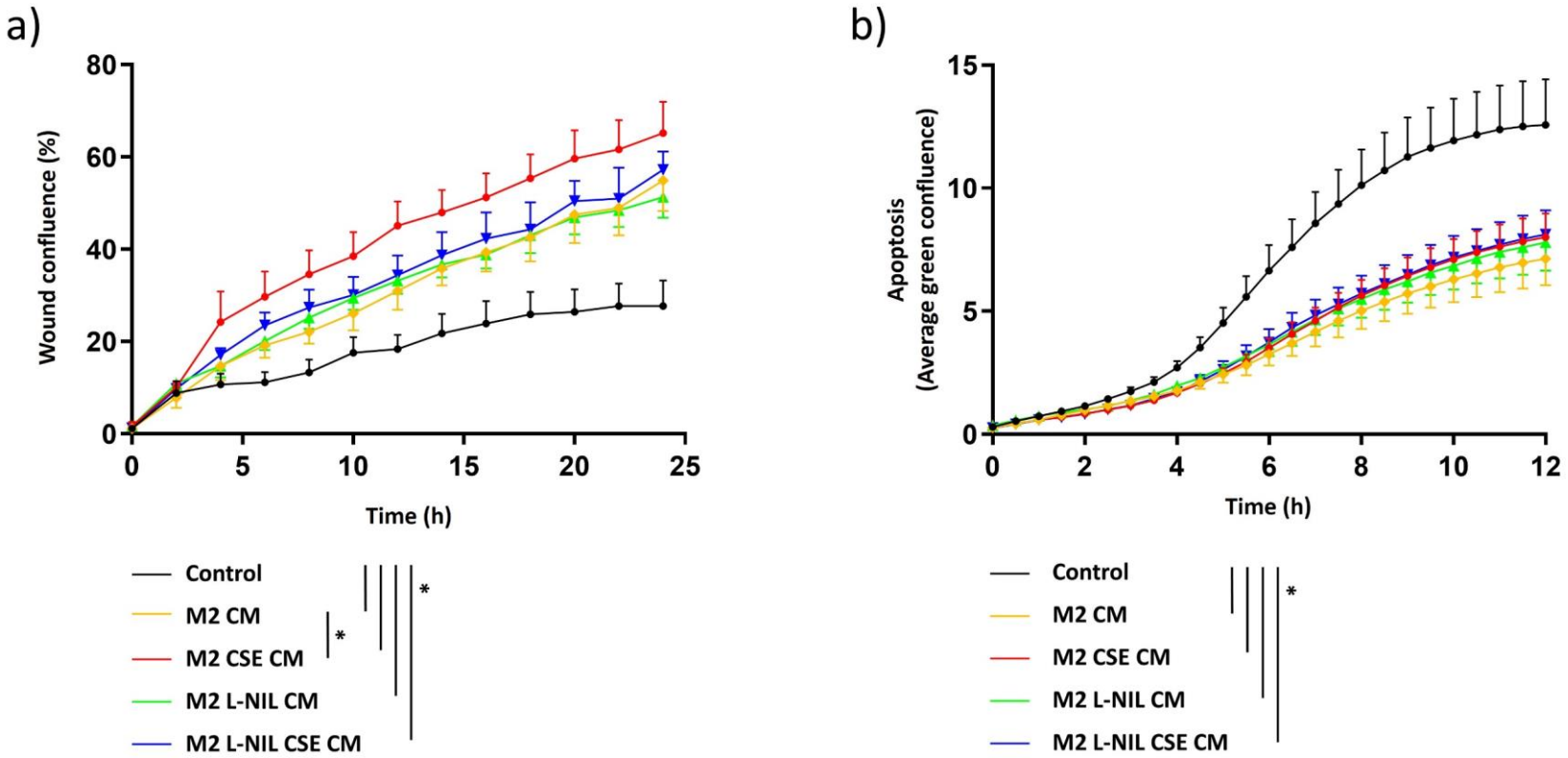

Figure S6: Investigation of the ERK pathway activation in co-cultured PASMC and mouse lung homogenates

a) Representative photos (upper panel) and Western blot analysis (lower panel) of ERK phosphorylation in PASMC co-cultured with CSE- and/or L-NIL treated M2 cells for 6h and 24h. Data are given as the ratio between phosphorylated and total ERK and standardized to control co-cultures (unexposed to CSE and untreated with L-NIL, n=4-5). PASMC shown on the upper panel are stained for phosphorylated extracellular signal-regulated kinase (ERK, green), α-smooth muscle actin (α-SMA, red) and counterstained with Hoechst (blue). Scale bars = 50 µm. b) Western blot analysis of ERK phosphorylation in PASMC co-cultured with M0 (left) and M1 (right) macrophages for 24h (n=4). Data are given as the ratio between phosphorylated and total ERK and standardized to control co-cultures (unexposed to CSE and untreated with L-NIL). c) Western blot analysis of the ERK phosphorylation in lung homogenates from animals exposed to smoke for 3 months and respective unexposed controls (n=6-7). Data are given as the ratio between phosphorylated and total ERK, standardized to control (unexposed WT mice). d) Schematic representation of the experimental design for assessing the effects of the extracellular signal-regulated kinase (ERK) inhibitor on the CSE-induced pro-proliferative signalling in co-cultures. Graphs show mean ± SEM. *$p < 0.05$. Two-way ANOVA (with Sidak´s multiple comparison post-hoc test for *in vitro* and Tukey´s multiple comparison post-hoc test for *in vivo* experiments) was used for statistical analysis.

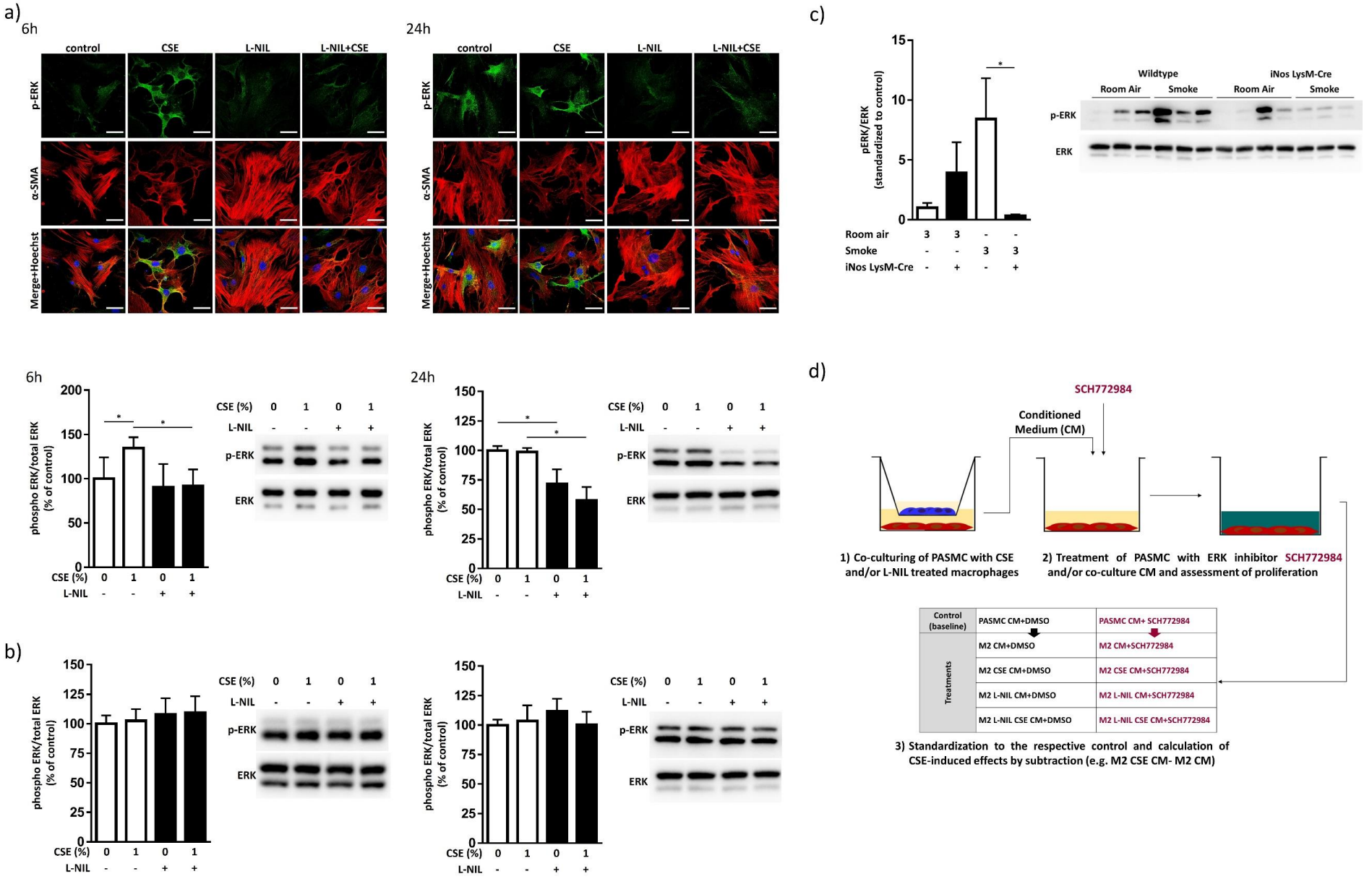
a)
6h
24h
control
CSE
L-NIL
L-NIL+CSE
p-ERK
α-SMA
Merge+Hoechst
phospho ERK/total ERK (% of control)
CSE (%)
L-NIL
ERK
b)
c)
pERK/ERK (standardized to control)
Wildtype
iNos LysM-Cre
Room Air
Smoke
Room air
iNos LysM-Cre
d)
SCH772984
Conditioned Medium (CM)
1) Co-culturing of PASMC with CSE and/or L-NIL treated macrophages
2) Treatment of PASMC with ERK inhibitor SCH772984 and/or co-culture CM and assessment of proliferation
Control (baseline)
PASMC CM+DMSO
PASMC CM+ SCH772984
Treatments
M2 CM+DMSO
M2 CM+SCH772984
M2 CSE CM+DMSO
M2 CSE CM+SCH772984
M2 L-NIL CM+DMSO
M2 L-NIL CM+SCH772984
M2 L-NIL CSE CM+DMSO
M2 L-NIL CSE CM+SCH772984
3) Standardization to the respective control and calculation of CSE-induced effects by subtraction (e.g. M2 CSE CM- M2 CM)